

On the Nonlinear Control of Hydraulic Servo-systems

Mohammad R. Sirouspour* and S. E. Salcudean**
Department of Electrical and Computer Engineering
The University of British Columbia
Vancouver, BC V6T 1Z4, Canada
E-mail: (*) *shahins@ece.ubc.ca* (**) *tims@ece.ubc.ca*

Abstract

In this paper the control problem of a hydraulic servo-system is addressed. The performance achievable by classical linear controllers, e.g. PD, are usually limited due to highly nonlinear behavior of the hydraulic dynamics. This paper adopts the backstepping design strategy to develop a Lyapunov-based nonlinear controller for a hydraulic servo-system. Load, hydraulic and valve dynamics are incorporated in the design process. An adaptation law is also proposed to deal with uncertainties in hydraulic parameters. The approach can be further extended to the control of hydraulically driven manipulators. Both simulation and experimental results are provided to show the effectiveness of the proposed method.

1 Introduction

Electrohydraulic actuators are widely used in industrial applications. They can generate very high forces, exhibit rapid responses and have a high power to weight ratio compared with their electrical counterparts. However, it is well-known that they exhibit a significant nonlinear behavior which makes the controller design a challenging task. Nonlinear flow/pressure characteristics, variations in the trapped fluid volume due to piston motion, and fluid compressibility are major sources of nonlinearity in the actuation system. There may be other factors such as transmission nonlinearities, flow forces and their effects on the spool position, and friction, all contributing to this nonlinear behavior.

The traditional and widely used approach to the control of electrohydraulic systems is based on the local linearization of the nonlinear dynamics about a nominal operating point [1]. Unfortunately, the nonlinear behavior of the system enforces the use of conservative loop gains which sacrifice the controller performance in favor of its robustness. [2] proposed the use of pressure feedback to improve the performance of classical PD controllers in hydraulic systems. [3],[4] and other papers have proposed adaptive control to cope with parameter variations in the linearized model of the system. The major disadvantage of this

approach is the lack of a global stability proof. Robust control design based on the linearized model of the system is another approach which has been followed in previous work, e.g. [5],[6]. In [7], [8], the variable structure control (VSC) strategy has been adopted for the control of hydraulic servo-systems. However, chattering in the control action, which is inherent in VSC, can easily excite high frequency modes and destabilize the system. Dynamic feedback linearization has recently been used in the literature to develop hydraulic actuator control systems. The idea was first introduced in [9],[10] and later followed in [11]. In particular, [11] proposed a force-based position control strategy. In most of these papers, either it is assumed that the valve is fast enough and its dynamics have been neglected, or unreasonable measurements such as acceleration have been introduced in the feedback control law. The above assumption is not always true, as valve dynamics can degrade the overall performance if neglected in the controller design. The force control problem of hydraulic actuators has been addressed in [12],[13],[14]. [12] developed a nonlinear adaptive force controller to be used in hydraulic active suspension systems. In [13],[14] a Lyapunov-based control design technique, that accounts for valve dynamics, was utilized to develop force tracking controllers for hydraulic actuators.

In this paper the *backstepping* approach [15] is employed to develop a Lyapunov-based position tracking controller for a hydraulic servo-system. The valve dynamics are included in the model. An adaptive version of the controller is also presented. The idea is an extension of what was proposed in [14] for force tracking to position tracking. A higher order valve dynamics is considered in this paper. The method can be extended to the control of hydraulically driven robotic manipulators.

The paper is organized as follows. In Section 2 the dynamic equations of the system under study are presented. The nonlinear controllers are developed in Section 3. In Section 4 simulation results are discussed. Section 5 presents the experimental results and finally conclusions are drawn in Section 6.

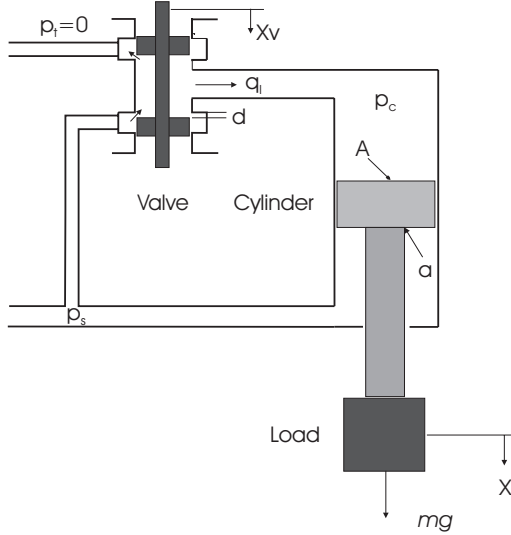


Figure 1 . A hydraulic actuator with three-way valve configuration.

2 System Dynamics

The differential equation governing the dynamics of the hydraulic actuator are given in [1]. The experimental hydraulic setup is connected in a three-way valve configuration as shown in Figure 1. For such a system, the control pressure dynamics are given by

$$\frac{V_t}{\beta} \dot{p}_c = q_l + c_l(p_s - p_c) - \dot{V}_t \quad (1)$$

where V_t is the trapped fluid volume in the control side, β is the effective bulk modulus, p_c is the control pressure acting on the control side, p_s is the supply pressure acting on the rod side, q_l is the load flow, and c_l is the coefficient of total leakage. V_t can be approximated by

$$V_t \approx A(x - L) \quad (2)$$

where A is the piston area, x is the actuator length and L is the actuator stroke length.

The load flow, q_l , is a nonlinear function of control pressure and valve spool position and is given by

$$q_l = \begin{cases} c(x_v - d)\sqrt{p_c} & x_v < -d \\ c(x_v + d)\sqrt{p_s - p_c} + c(x_v - d)\sqrt{p_c} & -d \leq x_v \leq d \\ c(x_v + d)\sqrt{p_s - p_c} & x_v > d \end{cases} \quad (3)$$

$$c = c_d w \sqrt{\frac{2}{\rho}}$$

where c_d is the effective discharge coefficient, w is the port width of the valve, ρ is the density of the fluid, d is the valve underlap length and x_v is the valve spool position. In the ideal case in which the valve dynamics can be

neglected, x_v is the control command. However, in practice, x_v is the response of the valve to a command signal u . In particular, in the system that we have experimented with, the valve dynamics can be considered to be a second order system:

$$\ddot{x}_v = -\omega_e^2 x_v - 2\zeta_e \omega_e \dot{x}_v + \omega_e^2 u \quad (4)$$

In our experimental setup, further described in Section 5, a single hydraulic actuator drives a mass connected to its rod end in the vertical direction. Thus, the load dynamics are

$$p_c A - p_s a = m\ddot{x} + f_f - mg \quad (5)$$

where m is the total mass of the actuator and the load, f_f is the friction force (a nonlinear function of the actuator velocity) and g is the gravitational acceleration. A is the area of the piston and a is the annulus area.

Equations (1),(4),(5) completely describe the fifth order nonlinear dynamics of the system under study. The corresponding state space representation of these dynamics follows. By defining

$$x_1 = x, x_2 = \dot{x}, x_3 = p_c, x_4 = x_v, x_5 = \dot{x}_v$$

one can write (assuming $c_l = 0$)

$$\begin{aligned} \dot{x}_1 &= x_2 \\ \dot{x}_2 &= \frac{A}{m} x_3 - \frac{1}{m} f_f(x_2) + g - \frac{a}{m} p_s \\ \dot{x}_3 &= -\frac{\beta x_2}{(x_1 - L)} + \frac{\beta}{A(x_1 - L)} q_c(x_3, x_4) \\ &\approx f_3(x_1, x_2) + g_3(x_1, x_3) x_4 \\ \dot{x}_4 &= x_5 \\ \dot{x}_5 &= -\omega_e^2 x_4 - 2\zeta_e \omega_e x_5 + \omega_e^2 u = f_5(x_4, x_5) + g_5 u \end{aligned} \quad (6)$$

3 The Controller Design

The nonlinear system described by (6) is in so called *strict feedback form*. This special form allows the use of the recursive backstepping procedure for the controller design [15]. The method basically provides a recursive framework to construct a Lyapunov function and corresponding control action for the system stabilization. In the rest of this section, this idea is adopted to design a nonlinear controller for position tracking in a hydraulic servosystem. [14] used a similar methodology for force tracking in hydraulic actuators.

3.1 Non-adaptive Case

First, the system parameter are assumed to be known. Let $e_i = x_i - x_i^d$, $i = 1, \dots, 5$ and $e = x - x^d$. The design procedure is started by defining the following Lyapunov-like function

$$V_1 = \frac{1}{2}m(x_2 - x_2^d)^2 + \frac{1}{2}k_1(x_1 - x_1^d)^2 \quad (7)$$

The derivative of (7) is given by

$$\begin{aligned} \dot{V}_1 = & (-f_f + Ax_3 + mg - ap_s - m\dot{x}_1^d)(x_2 - x_2^d) \\ & + k_1(\dot{x}_1 - \dot{x}_1^d)(x_1 - x_1^d) \end{aligned} \quad (8)$$

With $x_3 = x_3^d + e_3$, and the following choice of x_3^d :

$$x_3^d = \frac{1}{A}[ap_s - mg + f_f + k_1(x_1^d - x_1) + k_2(x_2^d - x_2) + m\dot{x}_1^d] \quad (9)$$

\dot{V}_1 becomes

$$\dot{V}_1 = -k_2e_2^2 + Ae_2e_3. \quad (10)$$

Now, in order to go one step ahead, V_2 is defined as

$$V_2 = V_1 + \frac{\gamma_3}{2}(x_3 - x_3^d)^2 \quad (11)$$

By taking the derivative of (11) and using (10)

$$\begin{aligned} \dot{V}_2 = & \dot{V}_1 + \gamma_3(x_3 - x_3^d)(\dot{x}_3 - \dot{x}_3^d) \\ & \dot{V}_1 + \gamma_3e_3(f_3 + g_3x_4 - \dot{x}_3^d) \\ = & -k_2e_2^2 + \gamma_3e_3\left(\frac{Ae_2}{\gamma_3} + f_3 + g_3x_4 + g_3e_4 - \dot{x}_3^d\right) \end{aligned} \quad (12)$$

If x_4^d is chosen as

$$x_4^d = \frac{1}{g_3}\left(-f_3 + \dot{x}_3^d - \frac{Ae_2}{\gamma_3} - k_3e_3\right), \quad (13)$$

then (12) is simplified to

$$\dot{V}_2 = -k_2e_2^2 - \gamma_3k_3e_3^2 + \gamma_3g_3e_3e_4. \quad (14)$$

Let V_3 be defined as follows

$$V_3 = V_2 + \frac{1}{2}\gamma_4(x_4 - x_4^d)^2. \quad (15)$$

By taking the derivative of V_3 , one may write

$$\begin{aligned} \dot{V}_3 = & \dot{V}_2 + \gamma_4e_4(x_5 - \dot{x}_4^d) \\ = & -k_2e_2^2 - \gamma_3k_3e_3^2 + \gamma_4e_4\left(e_5 + x_5^d - \dot{x}_4^d + \frac{\gamma_3}{\gamma_4}g_3e_3\right) \end{aligned} \quad (16)$$

(16) suggests the following choice of x_5^d

$$x_5^d = \dot{x}_4^d - \frac{\gamma_3}{\gamma_4}g_3e_3 - k_4e_4, \quad (17)$$

which renders \dot{V}_3 into

$$\dot{V}_3 = -k_2e_2^2 - \gamma_3k_3e_3^2 - \gamma_4k_4e_4^2 + \gamma_4e_4e_5. \quad (18)$$

Finally, V_4 is defined to be

$$V_4 = V_3 + \frac{\gamma_5}{2}(x_5 - x_5^d)^2. \quad (19)$$

By taking the derivative of (19), one may write

$$\begin{aligned} \dot{V}_4 = & \dot{V}_3 + \gamma_5e_5(f_5 + g_5u - \dot{x}_5^d) = \\ & -k_2e_2^2 - \gamma_3k_3e_3^2 - \gamma_4k_4e_4^2 + \gamma_5e_5\left(f_5 + g_5u - \dot{x}_5^d + \frac{\gamma_4}{\gamma_5}e_4\right) \end{aligned} \quad (20)$$

If the control u is synthesized as

$$u = \frac{1}{g_5}\left[-f_5 + \dot{x}_5^d - \frac{\gamma_4}{\gamma_5}e_4 - k_5e_5\right] \quad (21)$$

then (20) is simplified to

$$\dot{V}_4 = -k_2e_2^2 - \gamma_3k_3e_3^2 - \gamma_4k_4e_4^2 - \gamma_5k_5e_5^2 \leq 0 \quad (22)$$

where

$$V_4 = \frac{1}{2}(k_1e_1^2 + me_2^2 + \gamma_3e_3^2 + \gamma_4e_4^2 + \gamma_5e_5^2) \quad (23)$$

and $k_1, k_2, k_3, k_4, k_5 > 0, \gamma_3, \gamma_4, \gamma_5 > 0$.

Note that (23) is a Lyapunov function for the system defined by (6), and the control law given by (9),(13),(17),(21) renders its derivative negative semidefinite. It is easy to show that $e = 0$ is the largest invariant set in $E = \{e \in \Omega | \dot{V}_4(e) = 0\}$. So, using LaSalle's principle [16], the tracking errors which include position and velocity tracking errors, converge to zero asymptotically.

The derivative terms in the control law (i.e. $\dot{x}_3^d, \dot{x}_4^d, \dot{x}_5^d$) can be obtained in terms of the system states. Nevertheless, the expressions are long and complex and may not be suitable for real-time implementation. Numerical differentiation was found to be adequate for this purpose.

3.2 Adaptive Case

In the controller development in the previous section, it was assumed that all of the system parameters are known. However, this assumption is not always true. Sometimes, it may be necessary to identify some of these parameters off-line or estimate them using on-line adaptive schemes. The proposed controller was found to be more sensitive to changes in the hydraulic parameters. Therefore, these parameters might be estimated on-line. To develop an adaptive version of the controller, equations (1)-(3) are rewritten in the following form:

$$\dot{x}_3 = \theta_1 f'_3 + \theta_2 g'_3 x_4 \quad (24)$$

where $\theta = [\beta \ \beta_c]^T$ is the actual parameter vector and $\hat{\theta}$ is its estimate, and

$$f'_3 = \frac{x_2}{x_1 - L} \quad (25)$$

$$g'_3 = \begin{cases} \sqrt{x_3}/(A(x_1 - L)) & x_4 < -d \\ (\sqrt{x_3} + \sqrt{p_s - x_3})/(A(x_1 - L)) & -d \leq x_4 \leq d \\ (\sqrt{p_s - x_3})/(A(x_1 - L)) & x_4 > d \end{cases} \quad (26)$$

Now, V_2 in (11) is redefined as

$$V'_2 = V_1 + \frac{\gamma_3}{2}(x_3 - x_3^d)^2 + \frac{1}{2}\gamma_{\theta_1}\tilde{\theta}_1^2 + \frac{1}{2}\gamma_{\theta_2}\tilde{\theta}_2^2, \quad (27)$$

where $\tilde{\theta} = \theta - \hat{\theta}$. The derivative of (27) is given by

$$\begin{aligned} \dot{V}'_2 = \dot{V}_1 + \gamma_3 e_3 (\theta_1 f'_3 + \theta_2 g'_3 x_4^d + \theta_2 g'_3 e_4 - x_3^d) \\ - \gamma_{\theta_1} \dot{\hat{\theta}}_1 \tilde{\theta}_1 - \gamma_{\theta_2} \dot{\hat{\theta}}_2 \tilde{\theta}_2 \end{aligned} \quad (28)$$

Let x_4^d be certainty equivalent to (13).

$$x_4^d = \frac{1}{\hat{\theta}_2 g'_3} \left[-\hat{\theta}_1 f'_3 + x_3^d - \frac{A}{\gamma_3} e_2 - k_3 e_3 \right]. \quad (29)$$

Similarly, V_3 is redefined as

$$V'_3 = V'_2 + \frac{1}{2}\gamma_4 e_4^2. \quad (30)$$

By taking the derivative of V'_3 and substituting x_5^d with the following expression

$$x_5^d = x_4^d - \frac{\gamma_3}{\gamma_4} \hat{\theta}_2 g'_3 e_3 - k_4 e_4, \quad (31)$$

it can be shown that

$$\begin{aligned} \dot{V}'_3 = -k_2 e_2^2 - \gamma_3 k_3 e_3^2 - \gamma_4 k_4 e_4^2 + \gamma_4 e_4 e_5 \\ + \tilde{\theta}_2 \left[\gamma_3 g'_3 e_3 e_4 + \frac{\gamma_3 e_3}{\hat{\theta}_2} \left(-\hat{\theta}_1 f'_3 + x_3^d - \frac{A}{\gamma_3} e_2 - k_3 e_3 \right) \right. \\ \left. - \gamma_{\theta_2} \dot{\hat{\theta}}_2 \right] + \tilde{\theta}_1 \left(\gamma_3 f'_3 e_3 - \gamma_{\theta_1} \dot{\hat{\theta}}_1 \right) \end{aligned} \quad (32)$$

The parameter adaptation laws are then chosen as

$$\dot{\hat{\theta}}_1 = \frac{\gamma_3}{\gamma_{\theta_1}} f'_3 e_3 \quad (33)$$

$$\dot{\hat{\theta}}_2 = \frac{\gamma_3 e_3}{\gamma_{\theta_2}} \left[\frac{1}{\hat{\theta}_2} \left(-\hat{\theta}_1 f'_3 + x_3^d - \frac{A}{\gamma_3} e_2 - k_3 e_3 \right) + g'_3 e_4 \right], \quad (34)$$

which render \dot{V}'_3 into

$$\dot{V}'_3 = -k_2 e_2^2 - \gamma_3 k_3 e_3^2 - \gamma_4 k_4 e_4^2 + \gamma_4 e_4 e_5. \quad (35)$$

The rest of the design is the same as in the nonadaptive case and will not be presented here. By following similar steps, the asymptotic convergence of the state tracking errors to zero could be shown.

4 Simulation Results

Simulations have been performed to investigate the performance of the proposed nonlinear controllers. The simulation results have also been used to tune the controller for the experimental studies discussed in the next section. The results obtained from simulation are presented in this section. The following values have been used for the system parameters.

$$\begin{aligned} A = 1.14 \times 10^{-3} \text{ m}^2, \quad a = 6.33 \times 10^{-4} \text{ m}^2, \quad L = 1.37 \text{ m}, \\ p_s = 1500 \text{ psi}, \quad d = 55.4 \times 10^{-6} \text{ m}, \quad c = 1.5 \times 10^{-4}, \\ \beta = 700 \text{ Mpa}, \quad m = 30 \text{ kg}, \quad \omega_e = 255 \text{ rad/sec}, \quad \zeta_e = 0.6 \end{aligned}$$

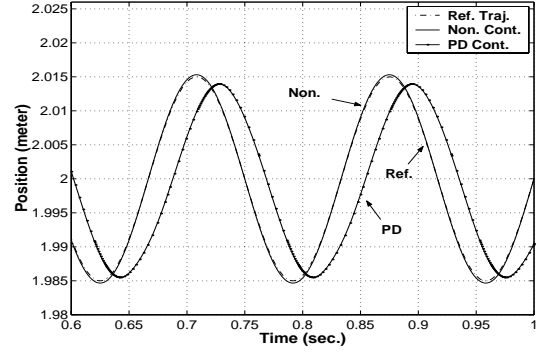


Figure 2 . The closed loop response to a sinusoidal reference trajectory with $f=6$ Hz (simulation).

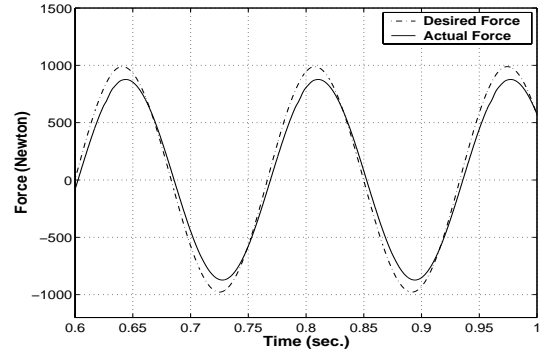


Figure 3 . Actuator output force profile for a sinusoidal position reference trajectory with $f=6$ Hz (simulation).

The friction was modeled as viscous damping with $b = 1000 \text{ N.s/m}$. The controller gains were chosen as $k_1 = 400000 \text{ N/m}$, $k_2 = 4000 \text{ N.s/m}$, $k_3 = 400 \text{ s}^{-1}$, $k_4 = 800 \text{ s}^{-1}$, $k_5 = 800 \text{ s}^{-1}$, $\gamma_3 = 10^{-10}$, $\gamma_4 = 15 \times 10^7$, $\gamma_5 = 15 \times 10^4$.

4.1 Nonadaptive Controller

The position tracking performance of the proposed controller (nonadaptive) is compared with a standard PD controller for a sinusoidal reference trajectory with $f = 6 \text{ Hz}$ in Figure 2. The PD controller has been optimized to reduce the position tracking error. The nonlinear controller clearly outperforms the linear one. It tracks the reference trajectory almost perfectly whereas the linear controller exhibits a significant phase lag.

In the controller design, the control pressure (or, equivalently, the actuator output force) was an intermediate virtual control command. Figure 3 presents the force tracking behavior of the actuator. The force tracking error, seen in this figure, is due to the velocity estimation error. Actually, the effect of piston motion in (1) is cancelled by (13) and because of the low compressibility of the fluid (huge β), the performance of force tracking is sensitive to this nonlinearity cancellation. To improve the performance, one

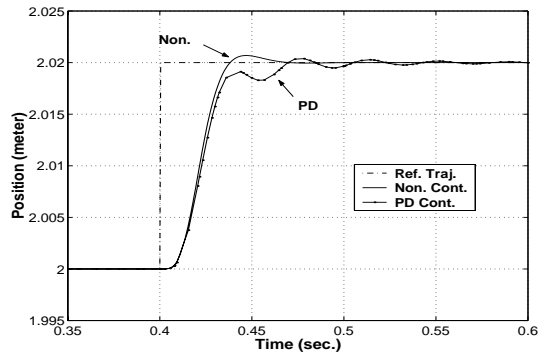


Figure 4 . The closed-loop step responses of the nonlinear and linear controllers (simulation).

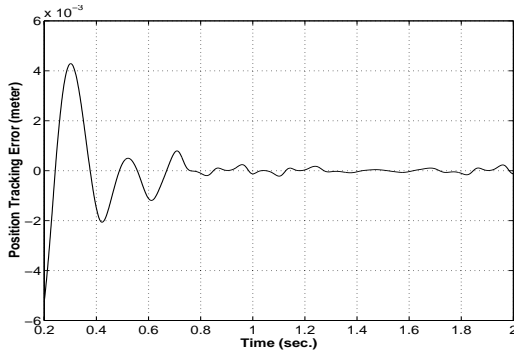


Figure 5 . Position tracking error profile for the adaptive controller (simulation).

should increase the pressure feedback gain (k_3). However, noise in the pressure loop can excite the high frequency modes and leads to system instability if a high pressure feedback gain is used. The step responses of the nonlinear and linear controllers are compared in Figure 4. Again, the proposed controller has better performance, especially a much smaller settling time compared with the PD controller. It should be pointed out that during the first rise phase both controllers saturate and therefore they behave almost identically.

4.2 Adaptive Controller

To investigate the effectiveness of the adaptive controller, another set of simulations were performed. The following adaptation gains were used to implement (33) and (34):

$$\gamma_{\theta_1} = 0.25 \times 10^{-14}, \quad \gamma_{\theta_2} = 0.25 \times 10^{-6}.$$

A multiple frequency reference trajectory was employed to excite the system. It was found that the controller is only sensitive to the ratio $c = \theta_2/\theta_1$, not the parameters themselves. In fact, the parameter estimations converge to values with the same ratio as the ratio of actual parameters, depending on their initial values. In the first simulation case, the initial estimates of the parameters were chosen to be 50% and 100% off from their actual val-

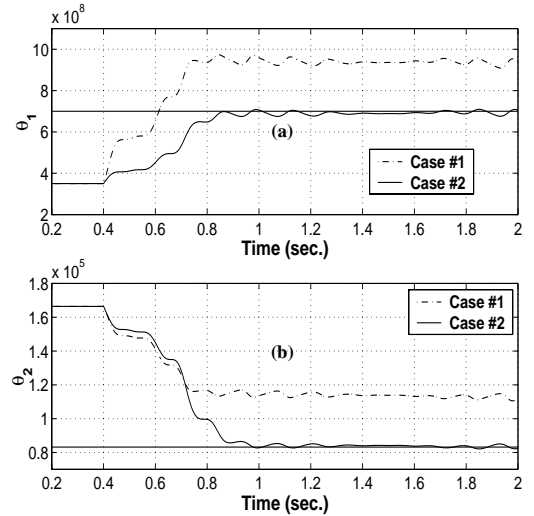


Figure 6 . The estimated parameters profiles, (a) θ_1 , (b) θ_2 . Solid lines show the actual values.

ues, respectively. The results are shown in Figure 6 (a, b). Solid lines represent the actual values of the parameters. In the second case, only one parameter was mismatched, and its adaptation law was active exclusively in each time. As a result the parameters converged to their actual values. The results are specified as Case 2 in Figure 6 (a, b). The tracking errors converge in both cases. Figure 5 shows the position tracking error in the first case.

5 Experimental Results

The proposed controller was also implemented in a laboratory hydraulic setup which was primarily developed to be used in a motion simulator [17]. The hydraulic actuation system is equipped with Rexroth 4WRDE three-stage proportional valves connected in a three-way configuration. Low friction Teflon seals are used in the hydraulic cylinders. Necessary modifications were made in order to perform single cylinder experiments, as seen in Figure 7. The computing setup consists of a VME-based real-time system running VxWorks on a Themis Sparc 5 board. Actuator length, valve spool position and supply and control pressures are measured through installed sensors. The schematic diagram of the controller is shown in Figure 8. All derivatives required in the control law were implemented by $\alpha - \beta$ filters [18]. The control update frequency was $f = 1$ kHz. Actual system parameters were all the same as those given in the simulation section. The controller gains were selected as:

$$k_1 = 400 \times 10^3 \text{ N/m}, \quad k_2 = 10000 \text{ N.s/m}, \quad k_3 = 100 \text{ s}^{-1}, \\ k_4 = 200 \text{ s}^{-1}, \quad k_5 = 200 \text{ s}^{-1}.$$

During the experiments, it was found that it is difficult to increase the pressure feedback gain k_3 . Increasing this

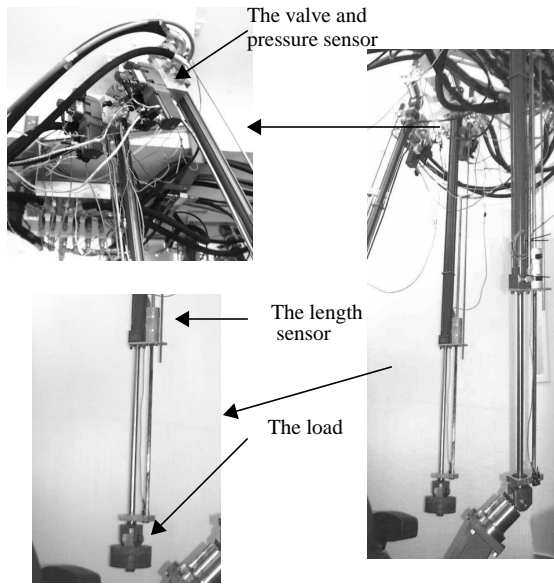


Figure 7 . The experimental setup.

gain allows the noise to excite the high frequency modes of the system and can lead to instability. Both adaptive and fixed-parameter controllers were implemented. However, it was observed that because of the relatively poor behavior of the pressure control loop, the use of the adaptive controller does not improve the position tracking performance significantly. The hydraulic parameters used in the nonadaptive controller were identified by an off-line least-squares estimation technique.

The nonlinear controller performance is compared with a standard PD controller in Figures 9, 11. The PD controller was tuned to obtain a good tracking performance while keeping the system stable. Figure 9 shows the position tracking for a reference trajectory with $f = 2$ Hz. The nonlinear controller clearly outperforms the PD controller despite its poor force tracking as shown in Figure 10. In Figure 11 the controllers are compared in tracking a 4 Hz reference position trajectory. Again the superiority of the nonlinear controller is observed.

6 Conclusions

In this paper the position control problem of a hydraulic actuator was addressed. The highly nonlinear behavior of the system limits the performance of classical linear controllers used for this purpose. The *backstepping* design strategy was adopted to develop a nonlinear controller that considers the valve dynamics. An adaptation algorithm was also proposed for on-line identification of hydraulic parameters. It was found that the proposed controller outperforms a tuned PD controller both in simulation and experiments. Despite the fact that the stiff pressure dynamics makes the inner pressure control loop sensitive to sys-

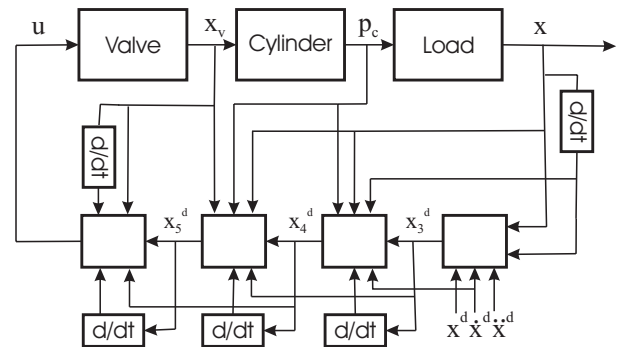


Figure 8 . The schematic diagram of the controller.

tem uncertainties, very good position tracking performance is obtained. The method has the potential to be extended to the control of hydraulic manipulators incorporating the actuator dynamics. This will be reported in future work.

Acknowledgments

The authors would like to thank Henry Wong and Simon Bachman for their contribution to this work. This project was supported by the Canadian IRIS/PREARN Network of Centers of Excellence.

References

- [1] H. E. Merrit, *Hydraulic Control Systems*, Wiley and Sons, New York, 1967.
- [2] D. Li and S. E. Salcudean, "Modeling, simulation, and control of a hydraulic stewart platform," in *Proc. IEEE int. Conf. Robotics and Automat.*, April 1997, pp. 3360-3366
- [3] J.S. Yun and H.S. Cho, "Adaptive model following control of electrohydraulic velocity control systems subjected to unknown disturbances," *IEE Proc.*, vol. 135, no.2, Mar. 1988, pp. 149-156.
- [4] J. E. Bobrow and K. Lum, "Adaptive, high bandwidth control of a hydraulic actuator," in *Proc. 1995 Amer. Contr. Conf. Evanston, IL: Amer. Automat. Contr. Council*, June 1995, pp. 71-75.
- [5] L. Laval, N. K. M'Siridi, and J. C. Cadiou, " H_∞ force control of hydraulic servo-actuator with environmental uncertainties," In *Proc. IEEE Int. Conf. Robotics and Automat.*, Minneapolis, Minnesota, April 1996, pp. 1566-1571.
- [6] H. Lu and W. Lin, "Robust controller with disturbance rejection for hydraulic servo systems," *IEEE Trans. Indust. Elec.*, vol. 40, pp. 157-162, Feb. 1993.
- [7] T. Chern and Y. Wu, "An optimal variable structure control with integral compensation for electrohydraulic position servo control systems," *IEEE Trans. Indust. Elec.*, vol. 39, pp. 460-463, Oct. 1992.
- [8] H. Yanada and M. Shimahara, "Sliding mode control of an electrohydraulic servo motor using a gain scheduling

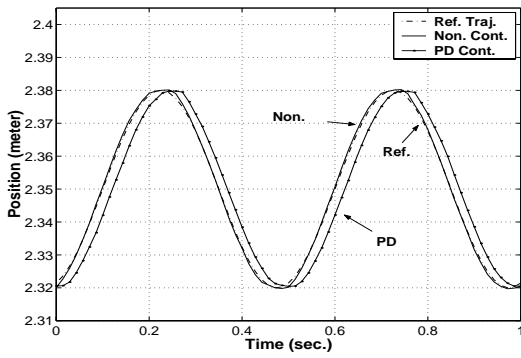


Figure 9 . The closed-loop response to a sinusoidal reference trajectory with $f=2$ Hz (experiment).

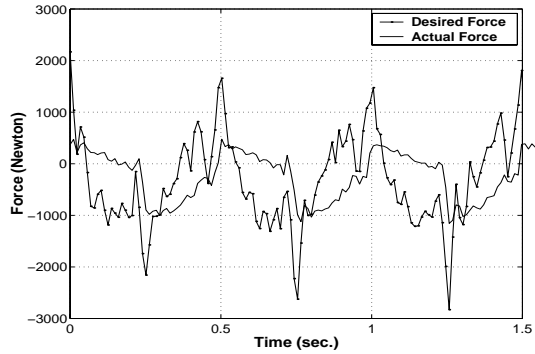


Figure 10 . The actuator output force profile for a sinusoidal position reference trajectory with $f=2$ Hz (experiment).

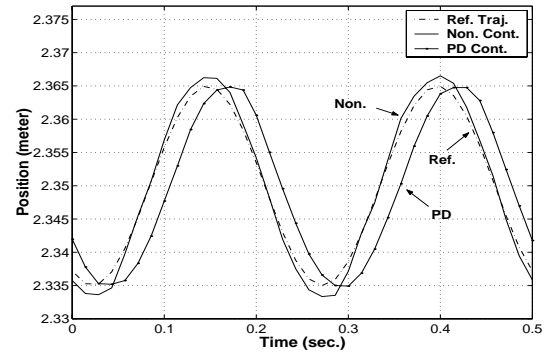


Figure 11 . The closed-loop response to a sinusoidal reference trajectory with $f=4$ Hz (experiment).

[16] J. E. Slotine and W. Li, *Applied Nonlinear Control*, Prentice-Hall Inc., New Jersey, 1991.

[17] S.E. Salcudean, P.A. Drexel, D. Ben-Dov, A.J. Taylor, and P.D. Lawrence, "A six degree-of-freedom, hydraulic, one person motion simulator," in *Proc. IEEE Int. Conf. Robot. Automat.* San Diego, CA, May 1994, pp. 2437-2443.

[18] Y. Bar-Shalom, T- Fortmann, *Tracking and Data Association*, Academic Press INC., 1988.

type observer and controller," In *Proc. Inst. Mech. Engrs.*, vol. 211, part I, 1997, pp. 407-416.

[9] H. Hahn, A. Piepenbrink, and K.D. Leimbach, "Input/output linearization control of an electro-servo-hydraulic actuator," In *Proc. IEEE Conf. Contr. Appl.*, UK, 1994, pp. 995-1000.

[10] G. Vossoughi and M. Donath, "Dynamic feedback linearization for electrohydraulically actuated control systems" *ASME J. Dyn. Sys., Meas., and Contr.*, vol. 117, Dec. 1995, pp. 468-477.

[11] G. A. Shol and J. E. Bobrow, "Experimental and simulations on the nonlinear control of a hydraulic servosystem," *IEEE Trans. Contr. Sys. Tech.*, vol. 7, pp. 238-247, Mar. 1999.

[12] A. Alleyne and K. Hedrick, "Nonlinear adaptive control of active suspensions," *IEEE Tran. Contr. Sys. Tech.*, vol. 3, pp. 94-101, March 1995.

[13] A. Alleyne, "Nonlinear force control of an electrohydraulic actuator," in *Proc. 1996 Japan/USA Symp. Flexible Automat.*, Boston, MA, 1996, pp. 193-200.

[14] R. Liu and A. Alleyne, "Nonlinear force/pressure tracking of an electrohydraulic actuator," in *IFAC world congress, 1999*.

[15] M. Krstic and I. Kanellakopoulos, and P. Koktovic, *Nonlinear and Adaptive Control Design*, Wiley and Sons, New York, 1995.